Electronic Supplementary Material (ESI) for ChemComm.

Supporting Information

A new benzimidazole based covalent organic polymer having high energy storage capacity

Bidhan C. Patra, Santimoy Khilari, Lanka Satyanarayana, Debabrata Pradhan and Asim Bhaumik*

Section	Content	Page No
S-1	Experimental	1
S-2	FT-IR & ^{13}C MAS NMR	2
S-3	FESEM Image	3
S-4	XPS plot of O1s for the TpDAB	3
S-5	Powder X-ray diffraction pattern of TpDAB	4
S-6	Pore size distribution of TpDAB from the BET analysis	4
S-7	Comparative study of specific capacitance of different electrode materials	5
S-8	Energy density and power density of present electrode material	6
S-9	References	7

Section S-1: Experimental

BICOP-1 material was synthesized via Schiff-base condensation polymerization protocol. The reaction was conducted with 1,3,5-triformyl-phloroglucinol (Tp: 0.063 g) and 3,3′-diaminobenzidine (DAB; 0.048 g) in mesitylene:dioxane (M:D=1:1) solvent in the presence of 0.5 mL 6 M acetic acid as catalyst. The reactants were first dispersed in a pyrex tube (8 inch long and 20 mm diameter) by sonication for 30 min to form a complete homogeneous mixture and then degassed through freeze-pump- thaw cycle for three times. Finally the tube was flame sealed and kept in 120 ^{0}C oven for 72 h. After 72 h, the deep red coloured material was filtered and washed with dioxane, water, and acetone, respectively and dried under vacuum at 120^{0}C for 6 h to obtain the benzimidazole based covalent organic polymer material TpDAB.

1,3,5-triformylphloroglucinol was prepared from phloroglucinol using an earlier reported procedure.[1] All other reagents and solvents were analytical grade and used without further purification. FT-IR spectra of the synthesized samples were recorded using a Nicolet MAGNA-FT IR 750 Spectrometer Series II. Solid state ^{13}C CP MAS NMR

spectrum of TpDAB was recorded in a 500 MHz Bruker Avance III spectrometer at a MAS frequency of 10 kHz. X-Ray diffraction patterns of the powder samples were obtained with a Bruker AXS D-8 Advanced SWAX diffractometer using Cu-Kα (0.15406 nm) radiation. N_2 adsorption/desorption isotherms of the sample was recorded using an Autosorb 1C (Quantachrome, USA) at 77 K. using NLDFT considering the carbon/slit-cylindrical pore model. Scanning electron microscopic analysis was performed with a JEOL JEM 6700F field-emission scanning electron microscope (FESEM). High resolution Transmission electron microscopy (HR-TEM) images of the synthesized polymer were obtained using a JEOL JEM 2010 transmission electron microscope operated at 200 kV. Electrochemical analysis was conducted in a standard three electrode arrangement with a 1 M Na2SO4 aqueous solution in a CHI 760 D electrochemical work station (CH instrument, USA). Active material coated glassy carbon electrode, Pt wire and a saturated calomel electrode (SCE) were considered as working, counter and reference electrodes, respectively. The active material slurry was prepared by dispersing appropriate amount of sample in ethanol followed by addition of 10 wt% polytetrafluoroethylene (PTFE) solution. The geometric surface area of glassy carbon electrode is 0.07 cm^2 and active materials loading measured to be 0.29 mg/cm^2. The cyclic voltammograms (CVs) were recorded with in a potential window of -0.2 to 0.8 V in the scan rate range of 2 to 100 mV/s. Galvanostatic charge discharge (GCD) activity of electrode material was studied with different constant current density in a potential window of -0.2 to 0.8 V. The electro chemical impedance (EIS) spectra were collected by applying a sinusoidal perturbation of 5 mV in a frequency domain 1 to 100 kHz.

Section S-2: FT-IR & ^{13}C MAS NMR

The FT-IR spectrum of the as-synthesized TpDAB is shown in Figure S1. The absence of C=O stretching frequency at 1639 cm-1 of Tp suggested complete consumption of trialdehyde in the formation of benzimidazole framework. This is also associated with the complete disappearance of IR stretching frequency corresponding to the N-H stretching band (3100-3300 cm-1) of the free amine of DAB. The characteristic peak for hydroxyl (-OH) functional group and the imines (C=N) functional group are absent in the FT-IR spectrum of TpDAB indicates the preferential existence of keto form rather than the enol form. Moreover, a sharp peak at 1598 cm-1 indicates the formation of C=C of the keto form rather the enol form due to keto-enol tautomerisation. Absence of imine (C=N) functional group clearly indicates the formation of imidazole ring rather the imine linked polymer. On the other hand, appearance of peak at ~3412 cm-1 indicates the N-H stretching frequency of the imidazole ring.[2] Due to the peak broadening in the extended polymeric structure of TpDAB, the carbonyl peak (C=O) at 1612 cm-1 was merged with C=C stretching band at 1598 cm-1. Other two peaks at 1447 and 1265 cm-1 could be attributed to the presence of aromatic C=C of benzidine ring and the C-N of imidazole ring respectively. The 13C CP-MAS NMR spectrum of the as-prepared TpDAB confirms the exhistance of keto form rather the enol form. The peak at 184 (C1) ppm is mainly due to the keto carbonyl carbon, which ruled out the enol form.[3] Absence of peak at 190 ppm for typical aldehyde (-CHO) carbon confirms total conversion of the starting material (Tp).[4] Appearance of peak at 148 ppm indicates the C-N of the imidazole ring rather the C=N at 165 ppm. Further the appearance of peak at 128 ppm (C4) is attributed to the junction carbon of the benzidine ring. Thus, the spectroscopic studies reveal that present TpDAB consists of benzimidazol linkage as illustrated in Figure 1a.

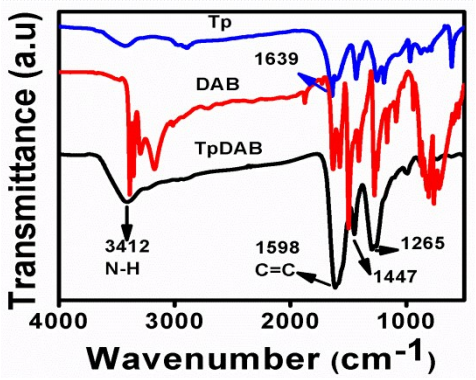

Figure S1.

Section S-3: FESEM Image

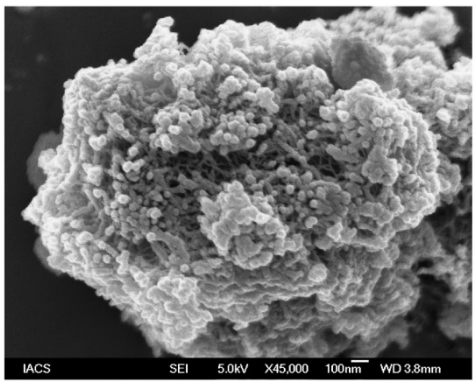

Figure S2.

Section S-4: XPS profile

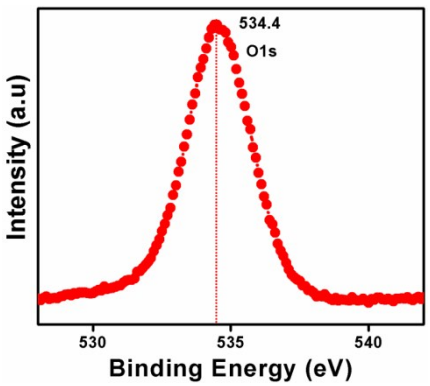

Figure S3. XPS profile of O1s in TpDAB.

Section S-5: Powder x-ray diffraction

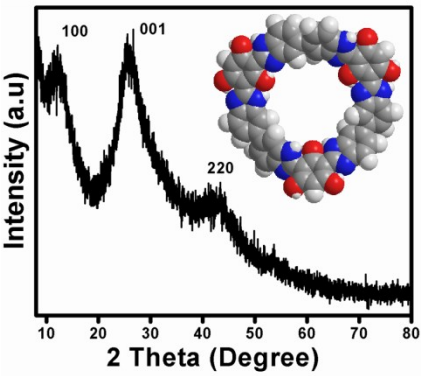

Figure S4. Powder X-ray diffraction pattern of TpDAB polymer.

Section S-6: Pore size distribution analysis

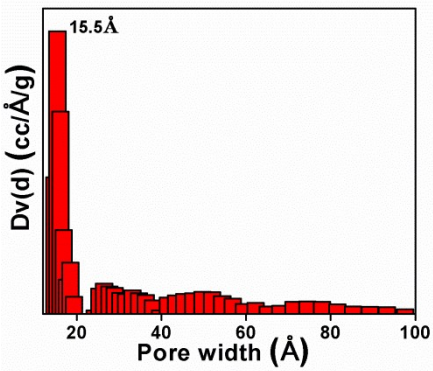

Figure S5. Pore size distribution plot of TpDAB.

Section S-7: Comparative study of electrochemical charge storage activity of different electrode materials

Table-1

Electrode material	Electrolyte	Specific capacitance (F g^{-1})	Current density (A g^{-1})	%Stability (cycles @ current density)	Reference
Porous triazine-based frameworks (PTF)	1-ethyl-3-methylimidazolium tetrafluoroborate	147 (PTF@500 ^{0}C) 151(PTF@700 ^{0}C)	0.1	85 (10000@10 A/g)	5
Graphene	30 wt.% KOH	150	0.1	90 (500 @ 0.1 A/g)	6
Hierarchically porous B doped carbons	1 M H_2SO_4	160	10 mV/s	-	7
Radical COFs (i)[TEMPO]100 %-NiP-COF (ii) [TEMPO]50 %-NiP-COF	0.1 M $(C_4H_9)_4NClO_4$ in CH_3CN.	(i)167 (ii) 124	0.1	(i) 81 (2000 @0.1 A/g) (ii) 70 (2000 @0.1 A/g)	8
Nitrogen-doped porous carbon foam	6 M KOH	210	0.5	100 (5000 @ 0.5 A/g)	9
Hierarchically porous carbon-AS-ZC-800	1 M H_2SO_4	251	0.25	-	10
MOF-derived nanoporous carbons	1 M H_2SO_4	251	0.5	92 (2000 @ 7.5 A/g)	11
Interconnected microporos carbon	1 M H_2SO_4	258	0.5	90 (5000@2 A/g)	12
MnO_2/carbon nanotube	polyvinyl alcohol/ H_2SO_4	324	0.5	82 (5000 @ 10 A/g)	13
Hierarchical Porous Carbon	1 M H_2SO_4	377	0.2	99.7 (5000 @1 A/g)	14
Nitrogen Enriched Porous Carbon Sphere	1 M H_2SO_4	388	1.0	98 (8000 @ 10 A/g)	15
Layered titanate ($H_2Ti_3O_7$) nanotubes	1 M $LiPF_6$ (non-aquaous)	414	0.5	82 (1000 @0.5 A/g)	16
PANI-doped graphene composite	2 M H_2SO_4	480	0.1	85 (5^{th} cycle @0.1 A/g)	17
Benzimidazole	1 M H_2SO_4	781	0.1	85 (2000 @100	18

grafted graphene		410	0.4	mV/S)	
TpDAB	**Aq. Na_2SO_4**	**432**	**0.5**	**93 (1000 @ 10 A/g)**	**Present work**

Section S-8: Energy density and power density of present electrode material

Energy density of electrode material was evaluated from following equation

$E = ½ .C_{sp}.V^2$ …….Equations S_1

where Csp and V refer specific capacitance and potential window respectively.

Power density was calculated using following equation

$P = E/t$

where 't' is time in hour.

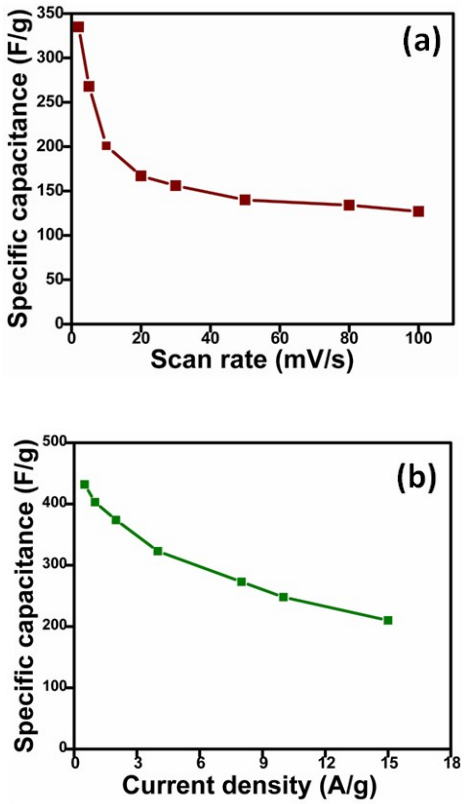

Figure S6. Specific capacitance vs scan rate (a) and specific capacitance vs current density (b) plots for TpDAB electrode.

Specific capacitance gradually decreases with increasing the scan rate and applied current density. This is due to restriction of ions insertion and slow redox kinetics on electrode surface at rapid scanning.

Section S-9: References

1. J. H. Chong, M. Sauer, B. O. Patrick, M. MacLachlan, Org. Lett. 2003, 5, 3823.

2. J. A. Asensio, S. Borrós, P. G. Romero, *J. Poly. Sci. A: Poly. Chem.,* 2002, **40**, 3703-3710.

3. S. Chandra, S. Kandambeth, B. P. Biswal, B. Lukose, S. M. Kunjir, M. Chaudhary, R. C. Babarao, T. Heine, R. Banerjee, *J. Am. Chem. Soc*., 2013, **135**, 17853-17861.

4. A. Modak, J. Mondal, V. K. Aswal, A. Bhaumik, *J. Mater. Chem.,* 2010, **20**, 8099-8106.

5. L. Hao, J. Ning, B. Luo, B. Wang, Y. Zhang, Z. Tang, J. Yang, A. Thomas, L. Zhi, J. Am. Chem. Soc., 2015, 137 , 219-225.

6. X. A. Du, P. Guo, H.H. Song, X.H. Chen, Electrochim. Acta., 2010, 55, 4812.

7. Y. B. Huang, P. Pachfule, J.K. Sun, Q. Xu, J. Mater. Chem. A, 2016, 4, 4273-4279.

8. F. Xu, H. Xu, X. Chen, D.Wu, Y. Wu, H. Liu, C. Gu, R.Fu, D.Jiang. 2015, 54, 6814-6818.

9. B. Liu, L. Zhang, P. Qi , M. Zhu, G. Wang, Y. Ma, X.Guo, H.Chen, B. Zhang, Z. Zhao, B. Dai , F. Yu , Nanomaterials, 2016, 6, 18.

10. A. J. Amali, J. K. Sun, Q. Xu, Chem. Commun., 2014, 50, 1519.

11. R. R. Salunkhe, Y. Kamachi, N. L. Torad, S. M. Hwang, Z. Sun, S. X. Dou, J. H. Kim , Y. Yamauchi, J. Mater. Chem. A, 2014, 2, 19848-19854.

12. D. Puthusseri, V. Aravindan, S.Madhavi, S. Ogale, Energy Environ. Sci., 2014, 7, 728-735.

13. W. Y. Ko, Y. F. Chen, K. M. Lu, K. J. Lin, Scientific Reports, 2016, 6, 18887.

14. J. S. Wei, H. Ding, Y. G. Wang, H. M. Xiong, ACS Appl. Mater. Interfaces, 2015, 7, 5811-5819 .

15. N. P. Wickramaratne, J. Xu, M. Wang, L. Zhu, L. Dai, M. Jaroniec, Chem. Mater., 2014, 26, 2820-2828.

16. J. Yang, L. Lian, P. Xiongab, M. Wei, Chem. Commun., 2014, 50, 5973-5975.

17. K.Zhang, L. L. Zhang, X. S. Zhao, J.Wu, Chem. Mater. 2010, 22, 1392-1401.

18. W. Ai, W. Zhou, Z. Du, Y. Du, H. Zhang, X. Jia, L. Xie, M. Yi, T. Yu, W. Huang, J. Mater. Chem., 2012, 23, 23439-23446.